Int. J. Electrochem. Sci., 10 **(2015)** 4029 - 4043

International Journal of
ELECTROCHEMICAL
SCIENCE
www.electrochemsci.org

Two-metal Corrosion of Casing Pipe Joint in CO_2/H_2S Environment

Chengqiang Ren[1,2,], Ming Zhu[2], Lei Du[3], Jianbo Chen[2], Dezhi Zeng[1], Junying Hu[1], Taihe Shi[1]*

[1] State Key Laboratory of Oil and Gas Reservoir Geology and Exploitation, Southwest Petroleum University, Chengdu, 610500, PR China
[2] School of Materials Science and Engineering, Southwest Petroleum University, Chengdu, 610500, PR China
[3] Southwest Branch of China Petroleum Engineering Co. Ltd., Chengdu, 610017, PR China
[*]E-mail: chengqiangren@163.com

Received: 31 January 2015 / *Accepted:* 5 March 2015 / *Published:* 23 March 2015

An investigation on the galvanic corrosion of dissimilar metals in CO_2/H_2S environments to simulate annulus pressure between casing and tubing string in sour gas well was conducted by methods of electrochemical measurement technique, high-pressure and high-temperature corrosion test and corrosion scale analysis. When C110 steel is coupled with 17-4 stainless steel or 718 nickel-base alloy, the galvanic effect is obviously found due to looser scale. The galvanic corrosion strongly depends on coupled material, environmental temperature, medium phase and annulus protection fluid. To mitigate galvanic corrosion, the two-metal casing joint should be placed in vapor or immersed in annulus protection fluid.

Keywords: CO_2/H_2S, galvanic effect, electrochemical measurement technique

1. INTRODUCTION

When a metallic contact is made between a more noble metal and a less noble one in an electrolytic, the corrosion rate will increase on the latter and decrease on the former. This phenomenon is called as two-metal corrosion or galvanic corrosion [1]. Many practical two-metal corrosion problems, including dissimilar-metal contact [2], dissimilar-metal welding joint [3], different-zone in weldment [4] and duplex-phase in metal [5], exist in various industries due to the requirements of cost, mechanical property, special demand, and so on.

In the oil and gas industry, carbon steel, low alloy steel, stainless steel and nickel-base alloy are under consideration according to ISO15156 when the engineers decide to make a materials selection for the tubes and pipes used in drilling, exploration and transportation. Stainless steel and nickel-base

alloy belong to corrosion-resistant alloy because of their low corrosion rate in CO_2/H_2S dissolved environments by comparing with carbon steel and low alloy steel. The high anticorrosion ability is attributed to alloying elements of Ni, Cr and Mo [6]. They improve the general, pitting and environmental crack corrosion resistance. However, their use is limited mainly because of the high cost. The dissimilar metals in tube and pipe strings are therefore always selected by accompanying special technology design based on the economic considerations in China. For example, the casing pipe in our investigating sour gas reservoir in Southwest China was composed of carbon steel (C110 steel) at upperpart of the well and corrosion-resistant alloy (17-4 stainless steel and 718 nickel base alloy) at underpart of the well, and the internal packer was set at the corrosion-resistant alloy part to ensure the upper annulus between casing and tubing string avoiding aggressive medium.

The annulus between casing and tubing string is always known as "A annulus". The problems of the leakage of casing or tubing string, poor sealing property of packer and the subsequent works let the gas and solution escape into the annulus which has high pressure, which results in an important phenomenon, namely, annulus pressure. It gives rise to challenge of well integrity damage [7].

Annulus pressure is a prevalent phenomenon in the worldwide. There is an increasing tendency for the A annulus pressure. More than 30% wells in the sour gas reservoir in Southwest China face the problem of A annulus pressure in recent years. The carbon steel/corrosion-resistant alloy joint is thus exposed in the brine containing acid gases of CO_2 and H_2S. One hazardous aspect is galvanic corrosion between the dissimilar metals contact.

Galvanic corrosion of carbon steel and stainless steel continues to be a concern. Literatures [8, 9] reported the galvanic corrosion between carbon steel and stainless steels (2205, 304L and 316L) in alkaline solution. They found galvanic effect between stainless steel and carbon steel was less obvious than the galvanic couple carbon steel and its rust. Chebahi et al [10] investigated marked effect of galvanic coupling between stainless steel (Fe-13%Cr) and carbon steel in NaCl solution at pH=3. Smailos et al [11] researched the galvanic corrosion between copper-nickel alloys and carbon steel in salt brine. Yin et al [12] discovered the galvanic effect of SM 80SS steel and Ni-based alloy G3 couple in NaCl solution in CO_2 containing environment. However, the understanding on the galvanic corrosion in CO_2 and H_2S environment needs to further efforts.

This work aims at the galvanic corrosion between carbon steel and corrosion-resistant alloy in CO_2 and H_2S environment, in order to know the risk of A annulus pressure. The investigations focus on influence of material type, environmental temperature, vapor-liquid phase and annulus protection fluid to the galvanic couple effect. Though area ratio is an important factor to galvanic corrosion, it is not under consideration in this work, because the casing joint is great enough regarding as 1:1 in the field application.

2. EXPERIMENTAL

2.1 Material and environment

To simulate the application in the sour gas reservoir in southwest China, C110 carbon steel, 17-4 stainless steel and 718 nickel-base alloy were used in the experiments. Their compositions with percentage in weight fraction are listed in Table 1.

Table 1. Compositions of alloys

Metal	Element concentration (%)										
	Ni	Cr	C	Si	Mn	P	S	Mo	Cu	Nb	Ti
17-4	3.83	16.20	0.07	0.77	0.64	0.03	0.03	-	2.32	0.56	-
718	51.2	18.41	0.04	0.11	0.10	0.01	0.01	2.90	-	-	1.02
C110	0.04	-	0.27	0.26	0.48	-	-	0.72	0.11	-	-

Two galvanic couples, C110/17-4 and C110/718, were studied to know the effect of materials to the galvanic corrosion. Before experiments, the surface of each metal was polished on silicon carbide paper, degreased by acetone, washed by water, rinsed by alcohol and dried by blow drier sequentially in order to obtain clean and smooth surface.

Table 2. Experimental conditions

Number	Experimental medium	Phase	Temperature
1	Formation water containing CO_2/H_2S	liquid	40 °C
2	Formation water containing CO_2/H_2S	liquid	80 °C
3	Formation water containing CO_2/H_2S	vapor	40 °C
4	Formation water containing CO_2/H_2S and annulus protection fluid	liquid	40 °C

The experimental mediums are the simulating formation water and the applying annulus protection fluid. The former was prepared by NaCl and distilled water to maintain 13.2 g L^{-1}. The latter was composed of 35% NaCOOH, 0.5% amphoteric polyacrylamide and 4% imidazoline. Four corrosion conditions, shown in Table 2, were investigated to understand the effect of environmental factors to the galvanic corrosion. Before experiments, the solution was adequately deaerated by N_2 gas bubble at least 6 h.

2.2 Galvanic couple

The diagrammatic sketches of galvanic couples in different measurements are presented in Fig. 1. In the solution environment, the galvanic couple was built by two parallel arranged metals in an electrical insulated fixture for galvanic current measurement. Their distance was 15 mm. The metals were covered by the insulating adhesive except the exposed part. The exposed area ratio of two electrodes in medium was 1:1. For corrosion rate measurement by weight loss, the assembling drawing

was changed. The support to the two metals was an electric metal. Also only 1:1 area ratio of two metals was maintained.

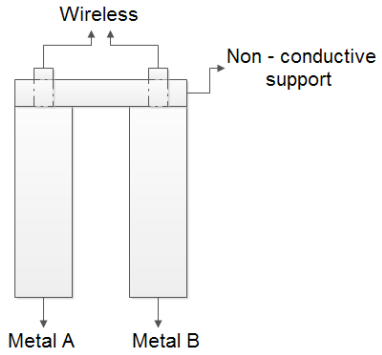

(a) Sample for galvanic current test in solution

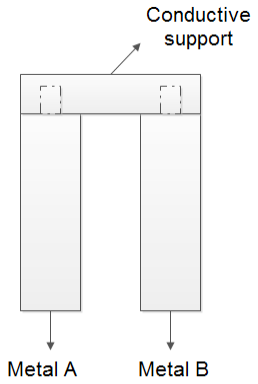

(b) Sample for weight loss in solution

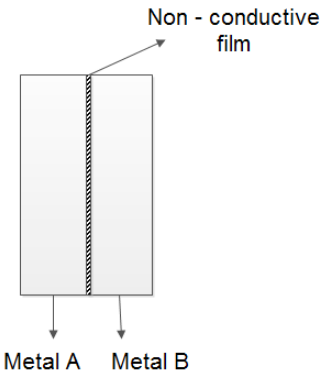

(c) Sample for galvanic corrosion in vapor

Figure 1. Sketch picture of specimen

In vapor environment for galvanic corrosion measurement, the two metals stood face to face, but there was a thin plastics film separating dissimilar electrodes.

2.3 Electrochemical measurement

The Model ZRA-2 galvanic corrosion tester was employed to perform the galvanic current test. The reference electrode was saturated calomel electrode in an electrolytic bridge. The galvanic current I_g was recorded for 7 days.

When potentiodynamic polarization and Mott-Schottky electrochemical techniques were operated, the classical three electrode cell was built, including a platinum plate counter-electrode, a saturated calomel reference electrode inserted in an electrolytic bridge and the researched metal electrode. The Autolab Model PGSTAT302N electrochemical potentiostat was used to carry out measurements. During Mott-Schottky measurement, the frequency was fixed at 1 kHz, and the potential scanned from −1000 to +500 mV by the rate of 10 mV s^{-1}. The potentiodynamic polarization was operated by a scan rate of 0.5 mV s^{-1}.

2.4 Weight-loss test

The corrosion rate of metal was obtained by weight loss test. The samples included galvanic couple and individual metal. The corrosion experiment was operated in the high temperature and high pressure autoclave. Every test was lasted for 7 days. The corrosion rate, *v*, was calculated by the equation (1):

$$v = \frac{8.76(m_0 - m_t)}{St\rho} \quad (1)$$

where, m_0 and m_t are weight of sample before experiment and weight after removal of corrosion scale, *S* is the exposed surface area, *t* is the corrosion time, and ρ is the density of metal.

2.5 Corrosion scale analysis

The surface morphology of the corrosion scale was observed on a JSM-6490LV scanning electron microscope, and the constituent elements in the scale were detected with the matching Model GENESIS 2000 XMS microscope's energy-dispersive X-ray spectroscopy accessory.

3. RESULTS AND DISCUSSION

3.1 Galvanic couple difference

Fig. 2 shows the galvanic currents of C110/17-4 and C110/718 couples in saturated H_2S and CO_2 brine water at 40 °C. The similar tendency of galvanic current with increasing exposed time was found for the two types of two-metal contact.

In the early half day, the galvanic current decreased very fast. The second great decreasing amplitude began after 2 days. During last 3 days, it maintained stable value. This should be explained by the contribution of corrosion scale on the anodic electrode. As we all know, the active metal acts as electrochemical anode in the galvanic corrosion, i.e, C110 in both couples. The corrosion scale on carbon steel in acid gas containing medium presents double-layer [13,14], which elevates the

resistance in the galvanic cell. The observed two decreasing currents are respectively caused by the formation of the inner layer and outer layer respectively.

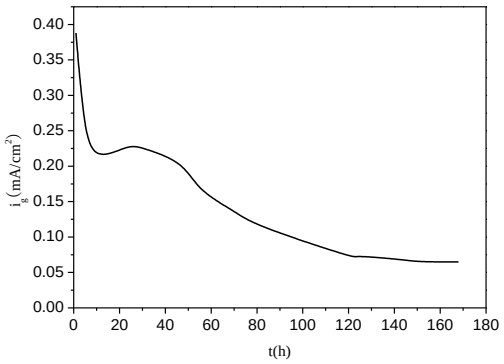

(a) C110/718

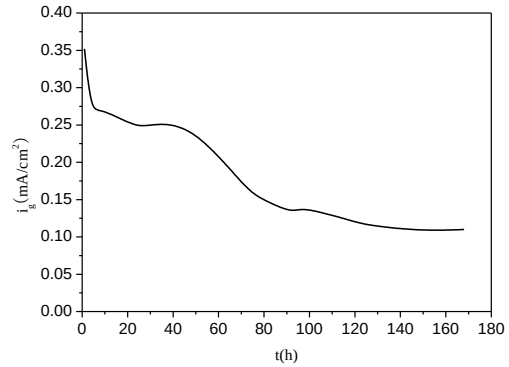

(b) C110/17-4

Figure 2. Galvanic currents of different couples in H_2S and CO_2 dissolved brine water at 40 °C

Table 3. Corrosion rate of C110 in brine water containing H_2S and CO_2 at 40 °C and 20 MPa

Couple	*V* (mm/a)	P_g
C110 alone	0.2561 (v_0)	1
C110/718	0.4863 (v_g)	1.90
C110/17-4	0.6610 (v_g)	2.58

The galvanic current of C110/17-4 couple is higher than that of C110/718 couple. This means C110 in C110/17-4 couple has higher corrosion rate. The general corrosion rate of C110 steel is listed in Table 3, which was obtained under the corresponding condition of 20 MPa (P_{H_2S} =1.5 MPa and P_{CO_2} =1.0 MPa) at 40 °C by weight loss method. The corrosion rate of C110 in C110/17-4 couple is 0.6610 mm/a, which is indeed higher than the value of 0.4863 mm/a of C110 in C110/718 couple. We define the galvanic effect (P_g) as equation (2).

$$P_g = \frac{v_g}{v_0} \times 100\% \quad (2)$$

Where, v_g is the galvanic corrosion rate, v_0 is the corrosion rate of steel alone. P_g represents the speedup ratio by the cathodic metal, that is to say, 17-4 and 718 give risk of galvanic corrosion to C110, but the former is more serious on the basis of highest P_g=2.58.

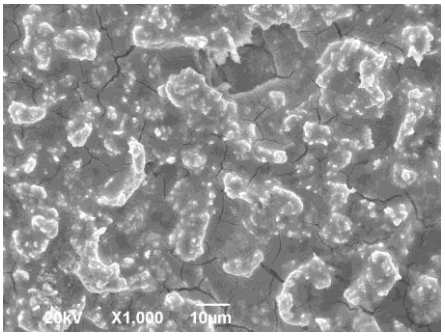

(a) C110 alone

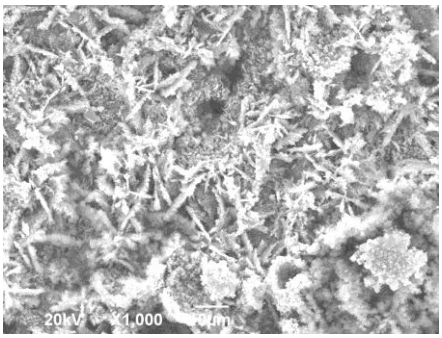

(b) C110 in C110/718 couple

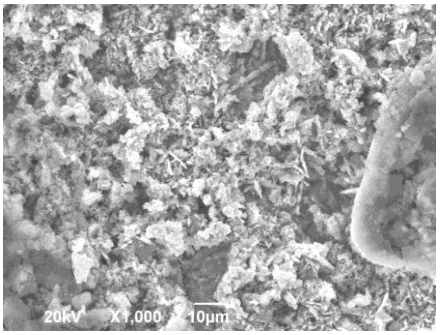

(c) C110 in C110/17-4 couple

Figure 3. Surface morphology of corrosion scale of C110 in brine water containing H_2S and CO_2 at 40 °C and 20 MPa

Fig. 3 shows the surface morphology of corrosion scale of C110 after taking out from solution in the autoclave. It is clearly seen the porous characteristics in the scales of galvanic couples, but the scale of C110 alone presents integrity structure. Elevated porosity in the scale is favor to the corrosion of steel [15].

3.2 Temperature difference

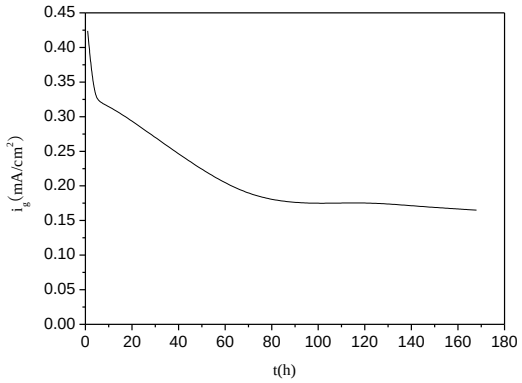

Figure 4. Galvanic current of C110/17-4 in H_2S and CO_2 dissolved brine water at 80 °C

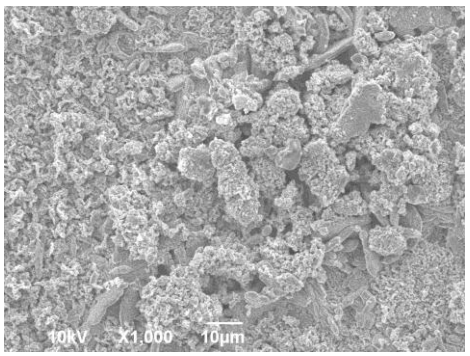

Figure 5. SEM of C110 in C110/17-4 couple in brine water containing H_2S and CO_2 at 80 °C and 20 MPa

In order to know the effect of temperature to the galvanic corrosion, the galvanic current of 17-4/C110 couple dependant on time at 80 °C is shown in Fig. 4. The stable current is obtained after 3 days exposure. This step is faster than that at 40 °C. The elevated temperature accelerates the formation of corrosion scale and enhances the galvanic effect. The steady-state current is clearly high than that at 40 °C.

Fig. 5 shows the surface morphology of C110 after corrosion under condition of 20 MPa (P_{H_2S} =1.5 MPa and P_{CO_2} =1.0 MPa) at 80 °C. The porous corrosion scale is observed. The impediment to the diffusion of aggressive ions becomes considerably less degree by comparing with the result at 40 °C. Therefore, the corrosion rate of C110 in C110/17-4 couple, 0.7433 mm/a, is elevated when temperature increases.

3.3 Medium phase difference

Fig. 6 shows the plot of galvanic current dependent time of C110/17-4 couple at 40 ºC in vapor. The galvanic corrosion occurs under thin liquid film, which is similar to the wet atmospheric

corrosion. Unlike the immersion corrosion in solution, the anodic reaction becomes difficult. It leads to lower galvanic effect, thus much smaller galvanic current vale is found. The corrosion rate of C110 in C110/17-4 couple, 0.0645mm/a, is evaluated by weight-loss method after 7 days' corrosion in vapor. It is only 10 percent of the corrosion rate in the solution.

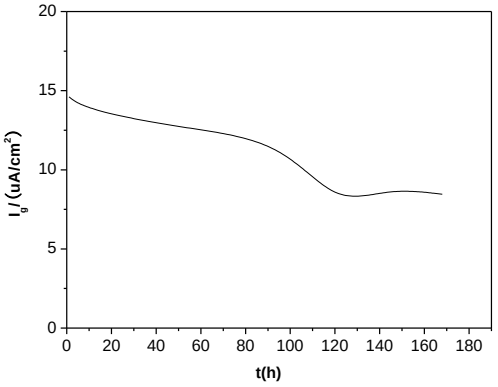

Figure 6. Galvanic current of C110/17-4 in vapor containing H_2S and CO_2 at 40 °C

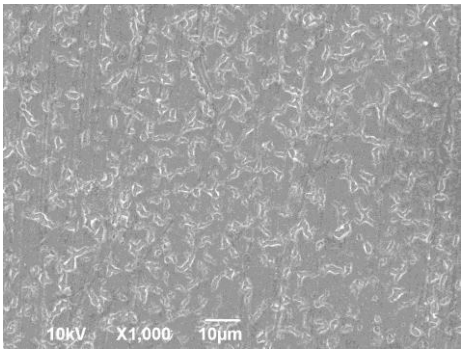

Figure 7. SEM of C110 in C110/17-4 couple in vapor containing H_2S and CO_2 at 40 °C and 20 MPa

SEM of the corrosion scale of coupled C110 at 40 ºC in vapor is presented in Fig. 7. The corrosion scale is thin and discontinuous. Corrosion is indeed slight. Therefore, the galvanic effect of C110/17-4 couple in vapor is extremely low. Based on these data, a method to protect the galvanic corrosion between C110 and 17-4 in the annulus can be suggested as avoiding the joint of dissimilar metals in solution, so the solution should be periodic discharged.

3.4 Role of annulus protection fluid

Figure 8 displays the dependence of galvanic current on time of C110 in C110/ 17-4 couple in brine water dissolved H_2S and CO_2 adding annulus protection fluid at 40 ºC. The galvanic current is marked mitigated to several μA. The stable current presents earlier than each above case in this investigation. At 1 day, annulus protection fluid reaches to excellent adsorption on the surface of steel

and elevates the pH value of solution, and it maintains long-term and high effectiveness. Slight corrosion is judged by the thin corrosion scale in Fig. 9. The corrosion rate of the coupled C110 is 0.0423 mm/a, which is much lower than the value in brine solution without annulus protection fluid. Thus, intermittent adding annulus protection fluid is an effective way for inhibiting galvanic corrosion of C110/ 17-4 joint.

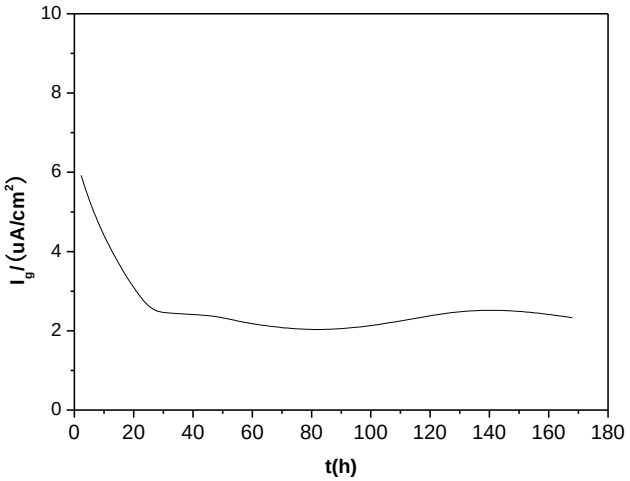

Figure 8. Galvanic current of C110/17-4 in H_2S and CO_2 dissolved brine water by adding annulus protection fluid at 40 °C

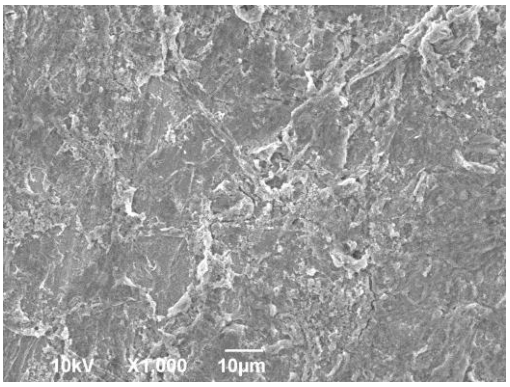

Figure 9. SEM of C110 in C110/17-4 couple in H_2S and CO_2 containing brine water by adding annulus protection fluid at 40 °C and 20 MPa

3.5 Galvanic corrosion mechanism

Fig. 10 shows the EDS of corrosion scale on C110 steel alone and with coupling after tested in high temperature and high pressure autoclave. The elements include Fe, S, C and O, and the former two are predominate. In acid gas containing solution, CO_2 dissolved in water produces $FeCO_3$, and H_2S leads to formation of FeS. The total reactions are given by equations (3) and (4).

$$Fe + CO_2 + H_2O \rightarrow FeCO_3 + H_2 \quad (3)$$

$$Fe + H_2S \rightarrow FeS + H_2 \quad (4)$$

The pressure fraction ratio of H_2S to CO_2 is 1.5 in these cases. The statistical data regarded that H_2S corrosion control the process when the ratio was higher than 1/200 [16].

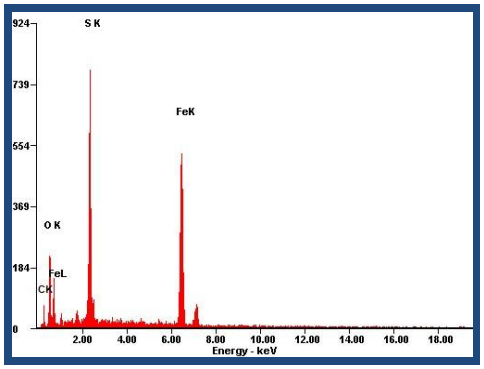

(a) C110 alone

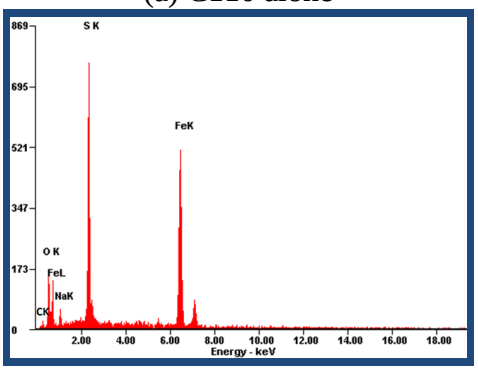

(b) C110 in C110/718 couple

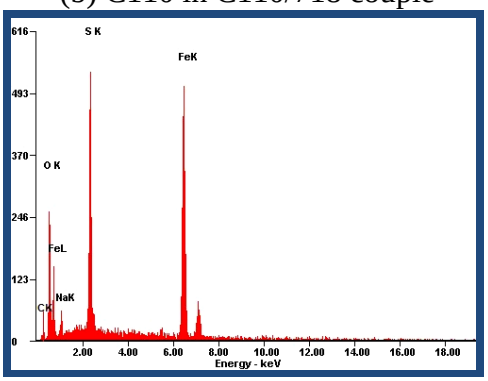

(c) C110 in C110/17-4 couple

Figure 10. EDS of corrosion scale of C110 in brine water containing H_2S and CO_2 at 40 °C and 20 MPa

The anodic reaction mechanism has been suggested by the adsorption of HS^- and the following electron transfer process [17]:

$$Fe + HS^- \rightarrow FeHS^-_{ads} \quad (5)$$

$$FeHS^-_{ads} \rightarrow FeS + H^+ + 2e \quad (6)$$

The cathodic reaction might be caused by:

$$2H_2S + 2e \rightarrow 2HS^- + H_2 \quad (7)$$

$$2HS^- + 2e \rightarrow 2S^{2-} + H_2 \quad (8)$$

$$2H^+ + 2e \rightarrow H_2 \quad (9)$$

The corrosion scale, iron sulfide, comes from two aspects. One is the primary product of anodic reaction, and the other is the secondary product when the primary products of anodic and cathodic reactions meet due to the neighboring sites. In fact, the iron sulfide is always non-stoichiometric, that is, Fe/S atom ratio does not equal to 1:1, and complex and indistinguishable products mix [18]. Generally, the secondary product can deposit at the defect of primary product to improve protection of corrosion scale to steel.

When C110 connects with 17-4 or 718, the cathodic reactions transfer from C110 surface to 17-4 surface or 718 surface, so the secondary product formation is inhibited. The corrosion scale on anodic C110 is looser by compared with C110 alone. This responds to the acceleration to corrosion. The main composition of corrosion product in galvanic corrosion is still iron sulfide.

It's well known that the potential difference causes galvanic corrosion. Generally, nickel-base alloy has more positive corrosion potential than stainless steel. However, 17-4 accelerates C110 corrosion considerably. 17-4 maybe has more efficient cathode for hydrogen evolution. The cathodic efficiency is an important factor to the galvanic corrosion in some industry applications [8].

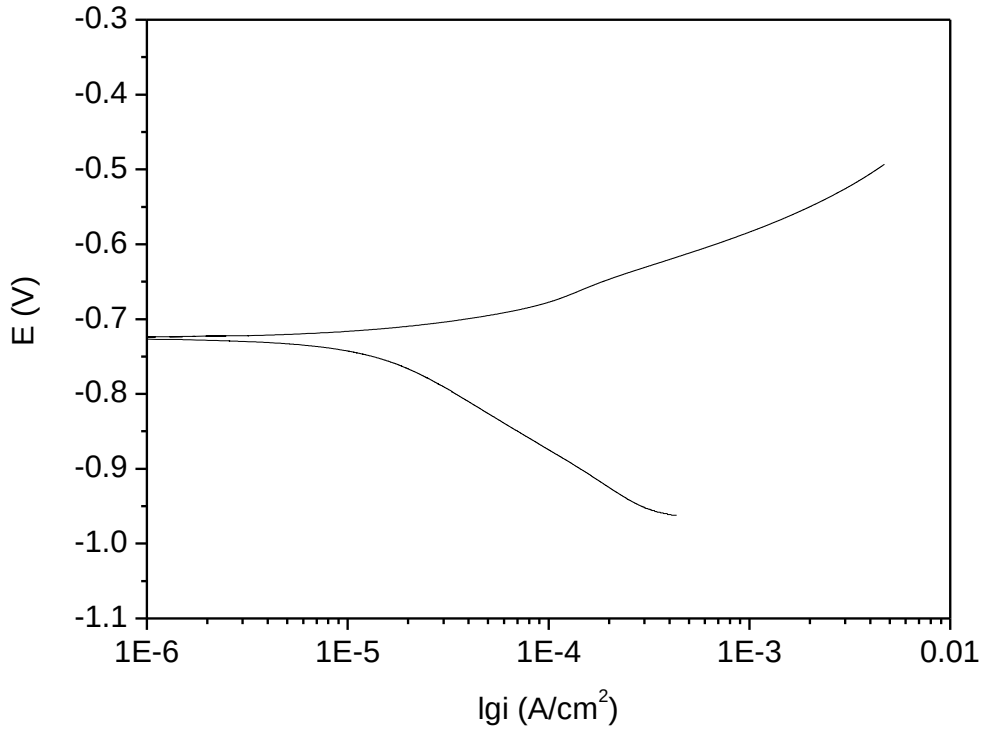

Figure 11. Polarization curve of C110 in H_2S and CO_2 dissolved brine water at 40 °C

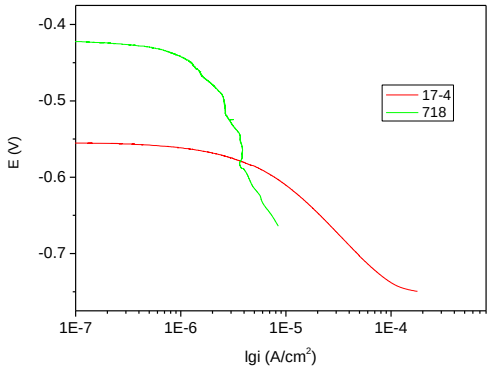

Figure 12. Cathodic polarization curves of 17-4 and 718 in H_2S and CO_2 dissolved brine water at 40 °C

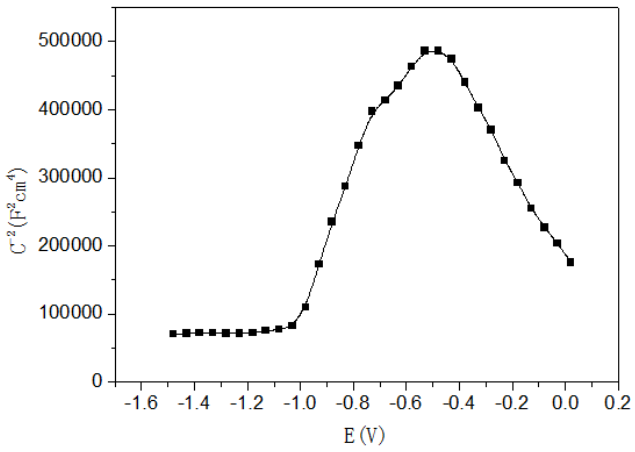

(a) C110 alone

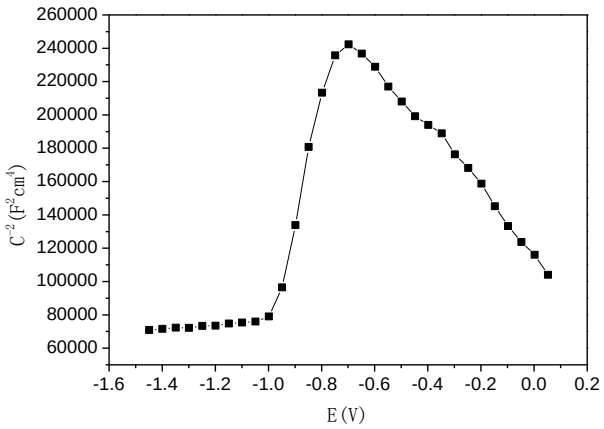

(b) C110 in C110/17-4 couple

Figure 13. Mott-Schottky plot of corrosion scale in H_2S and CO_2 dissolved brine water at 40 °C

Fig. 11 shows the polarization curve of C110 in H_2S and CO_2 dissolved brine solution at 40ºC. C110 corrosion is controlled by the cathodic reaction process rather than anodic one because of cathodic steeper linear section. It indicates the difficulty of hydrogen evolution on cathodic material greatly determines the galvanic corrosion of C110 when the galvanic coupling is connected. For this purpose, both 718 and 17-4 were measured for their polarization behaviors. The cathodic plots are particularly paid attention as shown in Fig. 12. It is found the cathodic contribution of 17-4 is greater than 718 in this condition due to the Tafel slope of -0.12 V/d for 17-4 but -0.30 V/d for 718.

Mott-Schottky plot is used to compare the electrical conductivity of corrosion scale covered on C110 when it is immersed alone and coupled with 17-4. The results are shown in Fig. 13. Whether C110 alone or C110 coupled with 17-4, bipolar semiconducting property presents for the corrosion scale. In the potential range of -0.1 V to 0.5 V, it plays n-type semiconductor on the basis of positive slope, but p-type semiconductor is found in higher potential range. The bipolar character may caused by obvious difference layers [19].

The dependence of E and C^{-2} for n-type semiconductor and p-type one are described by equations (10) and (11) [20]:

$$\frac{1}{C_{SC}^2} = \frac{2}{\varepsilon_0 \varepsilon_r N_D A^2}\left(E - E_{FB} - \frac{kT}{e}\right) \quad (11)$$

$$\frac{1}{C_{SC}^2} = -\frac{2}{\varepsilon_0 \varepsilon_r N_A A^2}\left(E - E_{FB} - \frac{kT}{e}\right) \quad (12)$$

Where ε_r is the relative dielectric constant of the specimen, ε_0 is the permittivity of free space (F cm^{-1}), e is the electron charge (C), A is the sample area (cm^2), N_D and N_A are the donor density (cm^{-3}) and acceptor density (cm^{-3}), E_{FB} is the flat band potential (V), k is the Boltzmann constant (J K^{-1}), and T is the absolute temperature (K). The electrical conductivity is proportional to concentration of charge carrier (N_D and N_A) in scale. N_D and N_A for each case are calculated and listed in Table 4.

Table 4. Charge carrier concentration in scale on C110 formed in brine water containing H_2S and CO_2 at 40 °C and 20 MPa

Sample	N_D/ cm^{-3}	N_A/ cm^{-3}
C110 alone	8.78×10^{22}	1.34×10^{23}
Coupled C110	1.53×10^{23}	4.39×10^{23}

When C110 is coupled with 17-4, the charge carrier increases in both two ranges of different semiconducting types by comparing with C110 alone. This discovers weaker protection of scale in C110/17-4 couple, which results in lower corrosion resistance of steel.

4. CONCLUSIONS

In this work, the galvanic effect of dissimilar-metal was researched by different experiments. Both 17-4 stainless steel and 718 nickel-base alloy give rise to galvanic corrosion risk to C110, but 17-4 has stronger acceleration than 718. When temperature increases from 40 ºC to 80 ºC, higher galvanic effect is found. If the dissimilar-metal is placed in vapor or immersed in annulus protection fluid, the galvanic effect is deeply mitigated.

ACKNOWLEDGEMENT
The authors thank financial supports by open fund (PLN1306) of State Key Laboratory of Oil and Gas Reservoir Geology and Exploitation (Southwest Petroleum University), National Natural Science Foundation of China (51374180).

References

1. Einar Bardal,Corrosion and Protection, Springer, 2004, 94.
2. M. Mouanga, M. Puiggali, B. Tribollet, V. Vivier, N. Pébère and O. Devos, *Electrochim. Acta* 88 (2013) 6.
3. P. Marashi, M. pouranvari, S. Amirabdollahian, A. Abedi and M. Goodarzi, *Mater. Sci. Eng. A* 480 (2008) 175.
4. M. G. Pujar, N. Parvathavarthini, R. K. Dayal and H. S. Khatak, *Int. J. Electrochem. Sci.* 3 (2008) 44.
5. Wen-Ta Tsai and Jhen-Rong Chen, *Corros. Sci.* 49 (2007) 3659.
6. X. H. Zhao, Y. Han, Z. Q. Bai and B. Wei, *Electrochim. Acta* 56 (2011) 7725.
7. Hasan Al Hosani, Abu Dhabi International petroleum exhibition and conference: Managing sustainable annulus aressures (SAP) in ADCO Field, *Abu Dhabi: Society of Petroleum Engineers*, 2005, Paper No. SPE-102052-MS.
8. S. Qian and D. Qu, *J Appl Electrochem.* 40 (2010) 247
9. C. M. Abreu, M. J. Cristobal, M. F. Montemor, X.R. Nóvoa, G. Pena and M. C. Pérez, *Electrochim. Acta* 47 (2002) 2271.
10. N. Chebahi, Ratiba Nedjar and M. Bounoughaz, *Asian J. Chem*. 20 (2008) 2563.
11. E. Smailos and B. Kienzler, *Corros.* 61 (2005) 230.
12. Z. F. Yin, M. L. Yan, Z. Q.Bai, W. Z. Zhao and W. J. Zhou, *Electrochim. Acta* 53 (2008) 6285.
13. D. G. Li, Y. R. Feng, Z. Q. Bai and M. S. Zheng, Appl. Surf. Sci. 253 (2007) 8371.
14. Meng Liu, Jianqiu Wang, Wei Ke and Enhou Han, *J. Mater. Sci. Technol.* 30 (2014) 504.
15. M. Gao, X. Pang and K. Gao, *Corros. Sci.* 53 (2011) 557.
16. S. Srinivasan, *Corros.* 14 (1999) 1168.
17. G. A. Zhang, Y. Zeng, X. P. Guo, F. Jiang, D. Y. Shi and Z. Y. Chen, *Corros. Sci.* 65 (2012) 37.
18. Pengpeng Bai, Shuqi Zheng, Hui Zhao, Yu Ding, Jian Wu and Changfeng Chen, *Corros. Sci.* 87 (2014) 397.
19. Ruijing Jiang, Changfeng Chen and Shuqi Zheng, *Electrochim. Acta* 55 (2010) 2498.
20. Z. Feng, X. Cheng, C. Dong, L. Xu and X. Li, *J. Nucl. Mater.* 407 (2010) 171.